Proceedings of 2013 ASME International Mechanical Engineering Congress and Exposition
IMECE 2013
November 15-21, 2013, San Diego, California

IMECE2013-66794

A MICROMECHANICAL MODEL FOR SHEAR-INDUCED PLATELET DAMAGE IN CAPILLARIES WITHIN GRAY MATTER

Daniel J. Sullivan
Rutgers, The State University of New Jersey
Piscataway, NJ, USA

Paul A. Taylor, PhD
Sandia National Laboratories
Albuquerque, NM 87185

Assimina A. Pelegri, PhD[1]
Rutgers, The State University of New Jersey
Piscataway, NJ, USA

ABSTRACT

In order to expand on potential injury mechanisms to the brain, a micromechanical structural representation of the gray matter must be developed. The gray matter contains a high volume of capillary vasculature that supplies the necessary oxygen required for maintaining healthy cell and brain function. Even short disruptions in this blood supply and the accompanying dissolved oxygen can lead to neuronal cell damage and death. It has been shown that increased shearing forces within the blood, such as those found near stents and artificial heart valves, can lead to platelet activation and aggregation, causing clots to form and potential disruptions in blood flow and oxygen distribution. Current macro-scale computational brain modeling can incorporate the larger main vasculature of the brain, but it becomes too computationally expensive to incorporate the smaller vessels. These larger scale models can be used to reveal how forces to the head are transmitted down to a scale slightly larger than the smallest capillaries within the gray matter. In order to investigate the response and potential damage to capillaries and platelets within the brain, a micromechanical computational model is developed incorporating the gray matter, capillaries, and blood, which is composed of plasma, red blood cells, and platelets. The red blood cells are a necessary component for the model for damage as it comprises almost half of the volume of blood and is the major contributor to the non-Newtonian behavior. The model combines both fluids and viscoelastic solid materials (the gray matter and the vascular wall). The deviatoric stress, strain and strain rate of the platelets in response to an externally applied load is measured and will determine the potential for platelet aggregation and clot formation. The micromechanical model is also used to provide verification and refinement for existing constitutive models for the gray matter used in meso- and macro-scale computational models.

KEYWORDS: Traumatic brain injury, finite element model, neurons, platelets, gray matter

1. INTRODUCTION

Traumatic Brain Injury (TBI) is a public health problem worldwide. Various studies throughout the past several decades have managed to shed light on some of the mechanisms of injury responsible for TBI. It has been well established that diffuse axonal injury, caused by various forms of mechanical trauma to the head, can lead to various cognitive and functional deficits. The cases of medium to major TBI can be easily diagnosed via various imaging techniques, such as Diffusion Tensor Imaging (DTI). These imaging techniques can reveal substantial damage to the axonal tracks within the brain. The problem of moderate to major TBI is an ongoing topic of study both experimentally and computationally. Various models for the whole head have been developed to create a computational basis for damage probabilities [1,2], and some progress has been made on micromechanical models for the white matter [3]. However, for cases of minor TBI, which make up approximately 75% of TBI cases [4], the exact mechanism for injury is a topic of ongoing research, and developing injury criteria and mechanisms could lead to benefits for patients and for general

[1] Corresponding Author, pelegri@jove.rutgers.edu

preventative measures. We are investigating the potential for a shear-induced platelet damage effect that could lead to localized clotting, ischemia, and hypoxia to the neuronal cell bodies. Within this study we develop a microscale, mechanical, finite element approach for studying the potential for shear-induced platelet damage within the gray matter of the brain.

The brain can generally be categorized into the white matter and the gray matter. The gray matter is primarily composed of neuronal cells, supporting glial cells, and a network of capillaries, which provide nutrition and oxygen to the brain. The white matter, composed primarily of glial cells and axons, which are projections off of the neuronal cell bodies, is responsible for communication between parts of the brain. DTI has been used to show that injuries to the head lead to damage to these axons, and various criteria have been developed in order to model and potentially prevent axonal injury.

While axons are easy to image, and are very important to the proper functioning of the brain, the gray matter plays a very important role as well. Few studies have been conducted on the potential damage mechanisms and diagnosis of gray matter injuries. Due to the increased vasculature present within the gray matter, we theorize that there is a potential for blood flow disruption caused by head trauma. It has been shown that even short 2-6 hour periods of focal ischemia can lead to cell death, lesions on the brain [5], and the presence of thrombi can persist for this amount of time or longer. This is the same mechanism that can lead to a stroke. It has also been shown that platelets are activated, in part, by shearing forces within the blood stream [6], and that this activation leads to further platelet activation aggregation, fibrin formation, and thrombus formation. It has also been shown that high shear flow conditions can sensitize platelets to subsequent normal flow conditions, and lead to increased activation for an hour or more [7]. Further, exposing platelets to shear of 108 Pa for as little as 7 ms has been shown to enhance platelet activation and coagulation [8].

Due to the small scales present, both physical and temporal, there is an inherent difficulty in the study of any such possible platelet activation. In addition, due to the natural thrombolysis mechanisms, there is a high likelihood that any observation of this effect in vitro would not be possible. In this case we turn to computational finite element modeling (FEM) techniques in an attempt to examine this scenario.

2 FINITE ELEMENT MODEL GENERATION

2.1 Model Geometry and Boundary Conditions

In order to simplify the computational model, we simulate a single capillary embedded within a gray matter matrix as a representative volume element (RVE). Within the capillary we have blood, composed of plasma, red blood cells (RBCs), and a representative platelet. For the purpose of this simulation we neglect the white blood cells due to their low volume concentration and large cell size. The geometries of the capillary are based on typical geometries for a capillary in the brain. Though there is a wide variance in the lumen diameter, from about 2 µm to 10 µm, the chosen lumen diameter of the capillary is 7 µm and we assign a wall thickness of 0.28µm [9]. The overall model has length of 18.75 µm and radius of 8 µm.

The platelet is modeled as a simple oblate spheroid with a major diameter of 3.52 µm and a minor diameter of 1.12 µm [10]. While it is typical for the platelet to be near the wall of the capillary in actual flow conditions, due to the axisymmetric nature of the model it is necessary to place the platelet along the middle of the capillary. It is believed that this will lead to lower shear forces and aggregation, and therefore a more conservative result [11].

The red blood cell deforms as it passes through the capillaries due the major diameter of the blood cell being greater than the lumen diameter of the capillary [12]. Due to this effect, a pre-deformed blood cell was used, based on the work of Bagchi [13]. This is an approximate representation of the parachute shape of the RBC.

The entire model is computed using Lagrangian elements because the short time scale of the simulation in general leads to low mesh distortions. The whole model, except for the red blood cell membrane, is modeled using both quadrilateral and triangular meshes. The red blood cell membrane is modeled using shell elements, and is present as a surface attached to the outer part of the red blood cell. The overall model contains 23,488 elements, and the general geometry can be seen in FIGURE 1.

The model is axisymmetric about the center of the capillary. Due to the size of the unit cell relative to the distance between capillary branches [14], we impose a symmetry condition on both ends of the RVE. In addition, the boundaries between the components of the model are considered to have frictionless contact, as a limiting case for interfacial conditions.

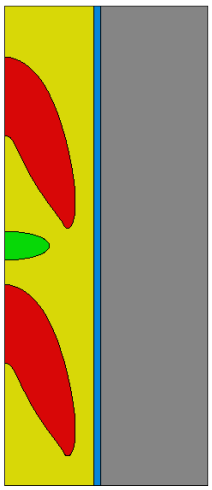

Figure 1. Undeformed model: gray - gray matter, blue - capillary wall, yellow - plasma, red - red blood cell, green - platelet

2.2 Material Models

In the following simulation loading rates are very high due to the load representing a simulated blast event. In order to accurately model these types of loads, a Mie-Grüneisen equation of state material is used to model the pressure response. This material model is appropriate for high strain rates and pressures, and is capable of dealing with the shock response of solid and liquid materials. The shock response of the material is related to the particle response by the Hugoniot equation,

$$U_S = C_0 + sU_P \tag{1}$$

and the overall Mie-Grüneisen form becomes

$$p = \frac{\rho_0 c_0^2 \eta}{(1-s\eta)^2}\left(1 - \frac{\Gamma_0 \eta}{2}\right) + \Gamma_0 \rho_0 E_m \tag{2}$$

where ρ_0,c_0, s, and Γ_0 are the mass density, y intercept and slope of the Us-Up Hugoniot representation, and the Grüneisen parameter, p is the pressure, E_m is the internal energy per unit mass, and η is the volumetric compressive strain. Because biological materials in general have a bulk material response very similar to that of water [15], the bulk response of all materials present, except for the red blood cell membrane due to shell element limitations, uses the following material properties for the volumetric response:

c_0	1.56 km/s
S	2.0
Γ_0	1.65

Densities of the various materials present are all near to that of water, with slight variations depending on the material. The densities used are from various sources [12,16–18], and can be found in the Table 1 below.

Table 1. Material properties of biological constituents

Material	Density (g/cm^3)
Gray matter	1.04
Capillary wall	1.04
Plasma	1.027
RBC Cytoplasm	1.027
RBC Membrane	1.15
Platelet	1.063

The material properties for platelets prior to activation are limited. The data available is primarily from micropipette aspiration [19,20]. Unlike the red blood cells, the platelet has a large amount of internal structures, so we use an isotropic homogeneous material property for it. Based on this, a shear modulus of 56.67 Pa was employed.

A number of studies have been done for the constitutive properties of gray matter [21–23]. For this research, we chose the work of Kaster et al. [21], which was based on nano-indentation of the tissue and FEM modeling to determine constitutive constants for various material models. A linearized version of the Yeoh hyperelastic model was used, giving a shear modulus for the gray matter of 370 Pa.

The red blood cells are specialized cells whose primary role is oxygen carrying capacity. They have a number of specialized characteristics that are beneficial for this purpose. Unlike most other cells, RBCs lack internal structure, and are essentially a hemoglobin containing fluid cytoplasm, surrounded by a flexible membrane. The membrane is composed of a number of layers that give the RBC the flexibility needed to pass through the smallest capillaries. Due to the structure of the membrane, it has anisotropic material properties. However, for this simulation, we are primarily interested in the effects on the platelet, so we assume an isotropic material with an effective thickness to provide the appropriate bending stiffness. We linearize the material properties found by Dao et al. [24] and Suresh et al. [25] using optical tweezers. In those works a neo-Hookean form of the strain energy potential is used, given by

$$U = \frac{G_0}{2}(\lambda_1^2 + \lambda_2^2 + \lambda_3^2 - 3) \tag{3}$$

where G_0 is the initial shear modulus and λ_1, λ_2, and λ_3 are the principal stretches. The material constants found were a bending stiffness of 2.0×10^{-19} N-m and an in-plane shear modulus of 5×10^{-6} N/m. The membrane shear modulus can be calculated from Equation (3) by taking the volume as constant and applying uniaxial strain, so that $\lambda_1 = \lambda$, and $\lambda_2 = \lambda_3 = \frac{1}{\sqrt{\lambda_1}}$, giving an energy function and nominal stress in the direction of strain as

$$U = \tfrac{G_0}{2}\left(\lambda_1^2 + \tfrac{2}{\lambda_1} - 3\right). \tag{4}$$

$$\sigma_{n1} = \frac{\partial U}{\partial \lambda_1} = G_0\left(\lambda_1 - \frac{1}{\lambda_1^2}\right) \tag{5}$$

Letting the current thickness be $h = h_0\lambda_3 = h_0\frac{1}{\sqrt{\lambda_1}}$, and $\sigma_n = \frac{F}{A} = \frac{F_1}{h_0(L_0)_2}$, we can find the uniaxial membrane stress,

$$\begin{aligned} T_1 &= \frac{F_1}{L_2} = \frac{F_1}{\lambda_2(L_0)_2} \\ &= \sqrt{\lambda_1}\frac{F_1}{(L_0)_2} = h_0\sqrt{\lambda_1}\sigma_n = h\lambda_1\sigma_n \\ T_1 &= h\lambda_1\frac{\partial U}{\partial \lambda_1} = G_0 h_0(\lambda_1^{1.5} - \lambda_1^{-1.5}). \end{aligned} \tag{6}$$

Then, as per Evans [26], with T_2=0, the membrane shear stress is given by

$$\begin{aligned} T_s &= 2\mu\gamma_s = \frac{\mu}{2}(\lambda_1^2 - \lambda_2^2) \\ T_s &= \frac{1}{2}(T_1 - T_2) = \frac{G_0 h_0}{2}(\lambda_1^{1.5} - \lambda_1^{-1.5}) \end{aligned} \tag{7}$$

and the instantaneous membrane shear modulus can be computed as

$$\mu(\lambda_1) = \frac{1}{2}\frac{\partial T_s}{\partial \gamma_s} = \frac{3G_0h_0(\lambda_1^{0.5} + \lambda_1^{-2.5})}{2(2\lambda_1 + \lambda_1^{-2})} \quad (8)$$

which gives an initial in-plane shear modulus of $\mu_0 = G_0h_0$, as in Mills et al. [27]. Given that the equation for initial bending stiffness is [12],

$$B = \frac{E_0{h_0}^3}{12(1-\nu^2)} \quad (9)$$

and that for an incompressible linear isotropic material, Young's modulus is related to the shear modulus by $E = 3G$ and Poisson's ratio $\nu = 0.5$, we can show that

$$B = \frac{G_0h_0^3}{3} \quad (10)$$

From solving with the equation for the in-plane shear modulus, we find that h_0=0.346µm and G_0=14.4Pa. Simulations were performed to replicate the experiments of Suresh et al. in order to confirm that a linearized model is usable for low strains.

While the viscous behavior of blood as a whole is non-Newtonian and highly shear-rate dependent, the individual fluids present, the plasma and the RBC cytoplasm, are effectively Newtonian fluids with a linear viscosity. The viscosity of the plasma is near that of water, with a viscosity of 1.06 cP [12]. The cytoplasm's viscosity is dependent on the hemoglobin concentration, with a typical value of 5.9 cP [28].

The capillary wall is composed of a single wall of endothelial cells. Due to the scarcity of information available for material properties for capillaries within the brain, the properties of pulmonary endothelial cells were used [29]. These give a shear modulus of 582 Pa. A summary of the material properties used can be found below.

Material	Properties
Gray Matter	G=370 Pa
Capillary wall	G=582 Pa
Plasma	η=1.06 cP
Cytoplasm	η=5.9 cP
RBC membrane	$B = 2.0 \times 10^{-19}$ N-m $\mu_0 = 5 \times 10^{-6}$ N/m
Platelet	G=56.67 Pa

Figure 2. Summarized Material Properties

2.3 Loading

The loads applied to the boundary are pure pressure loads along the edge opposite the axis of symmetry. These pressure loads are based on the work of Taylor, et al.[2], and are the pressure loads found within the thalamus, a region of primarily gray matter, when the model is exposed to a 360 kPa shock wave impinging on the side of the head. The peak overpressure found within the thalamus is approximately 345 kPa, followed by a -100 kPa underpressure. This loading can be found in FIGURE 3.

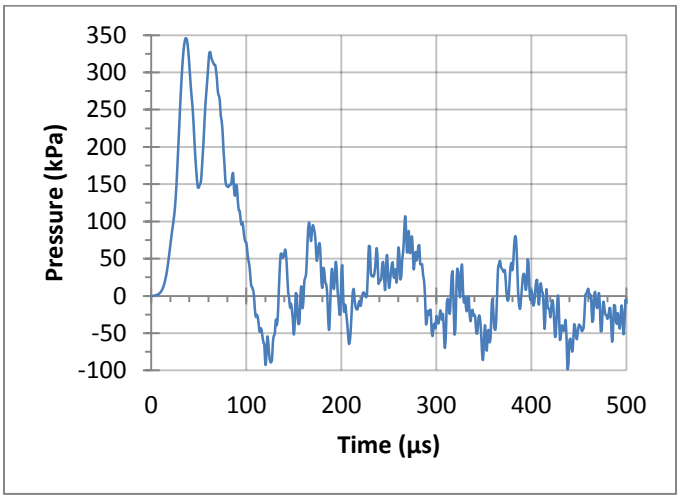

Figure 3. Pressure loading in thalamus showing first 500 µs (From Taylor, et. al)

3 RESULTS

Simulation was performed using Abaqus/Explicit with 23,488 elements on eight processors, with 20 µs of real time taking approximately 4 hours to simulate. Stability of the solution was monitored, and the simulation was stopped after slightly over 20 µs when mesh distortions lead to errors. Stresses and strains were recorded, and a volume averaged von Mises stress and in-plane shear stress were calculated and plotted (FIGURE 4). Maximum von Mises stress occurred at approximately 18 µs and was found to be 54.4 Pa, whereas shear stress maximum was 16.7 Pa. Von Mises stress at 18 µs is plotted in FIGURE 5. During the simulation time period, applied pressure loads reached a maximum of 69.5 kPa.

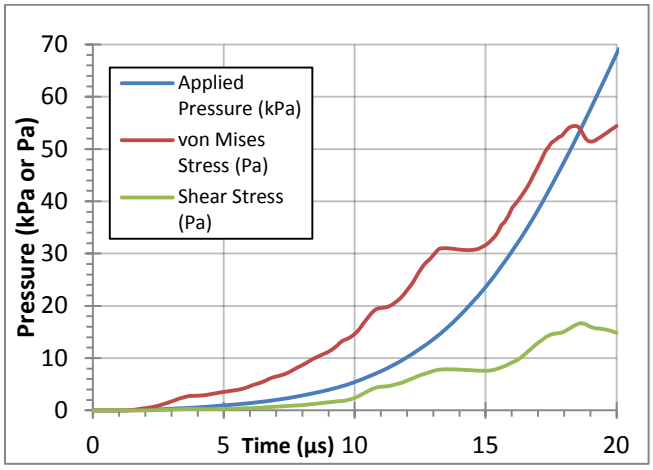

Figure 4. Resultant average shear and von Mises stress for platelet from pressure loading to RVE

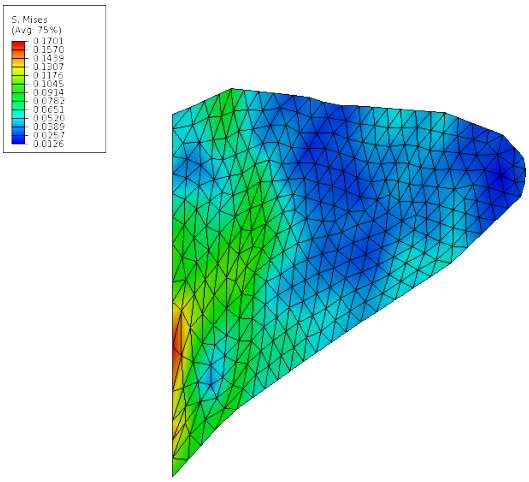

Figure 5. Von Mises stress experienced by platelet at 18 μs, ranging from 12.6 to 170.1 Pa

4 DISCUSSION

Shear stress develops within the platelet even though only pressure loads are applied to the RVE, due to mismatches in shear responses of the material, and the geometry of the RVE. Due to these effects, the shear stress within the platelet reaches relatively high levels even with applied loads only reaching approximately 20% of maximum loading.

Considering the platelet damage due to shearing results found by Wurzinger et al. [8], one can deduct that experimentally significant platelet activation effects occurred after a 7ms exposure to 108 Pa. Because this was done via Couette viscometry a hypothesis of uniform shear stress throughout the flow can be made, and therefore an average shear stress for the platelets of 108 Pa can be assumed. If one employs the above as a damage criterion, we can deduce that the platelets have only reached 15.6 % of that necessary for activation. However, it is important to note that the stress conditions of our simulation only reached 20% of maximum before being terminated due to mesh distortion. Since our predicted stress levels increase monotonically, it is possible that the shear stress will approach the threshold level for platelet activation if the simulation could be carried out to 100 μs or better. In addition, there is likely a delayed shear response due to the viscosities present within the simulation, which could lead to a higher average shear stress occurring after the pressure peak. During a blast injury, the strain rates present can be very high, on the order of 10^6 s^{-1}. Currently, to the best of the authors' knowledge, there does not appear to be any research on strain rate dependent platelets. However, other biological materials, such as neurons, experience damage related to strain rate [30], so a strain rate effect for platelets is a likely prospect as well.

There is also a possibility of damage based on a pure pressure response, similar to that found by Jérusalem et al. [31] for neuronal cells. That simulation was conducted on a much shorter time scale, 150 ns, and indicated a possibility for neuronal damage even at that time scale. An investigation of this potential damage mode would be of value for platelets, and will be pursued in future studies.

In addition, future work will be performed in order to provide a homogenized material model for the gray matter for use in large scale head models. This process is accomplished by applying various loadings to the RVE, such as tension, shear, and compression, and observing the mechanical response of the material. This response can then be incorporated into an anisotropic, non-linear material model.

5 CONCLUSIONS

In this work, a continuum based, finite element model for a platelet within a capillary embedded in gray matter was developed. A pressure load was applied to the model, and shear stress was recorded. Based on this work, there is some evidence for a potential shear stress platelet activation effect for a blast induced TBI.

The model revealed increasing deviatoric stress within the platelet under blast loading conditions. It successfully captures some of the possible injury mechanisms for platelets, and is a novel computational model for platelet damage. Further research both experimentally as well as computationally is needed to determine if stress and strain criteria for damage are met for the platelets, as well as determine what those criteria would be.

ACKNOWLEDGEMENTS

The authors would like to acknowledge the financial support of NSF, CMMI division for the Award 1000450 and the kind encouragement of the program manager Dr. Dennis Carter. The authors would also like to gratefully acknowledge the help and data provided by Dr. Prosenjit Bagchi.

Sandia National Laboratories is a multi-program laboratory managed and operated by Sandia Corporation, a wholly owned subsidiary of Lockheed Martin Corporation, for the United States Department of Energy's National Nuclear Security Administration under contract DE-AC04-94AL85000.

REFERENCES

[1] Zhang L., Bae J., Hardy W. N., Monson K. L., Manley G. T., Goldsmith W., Yang K. H., and King A. I., 2002, "Computational study of the contribution of the vasculature on the dynamic response of the brain," Stapp Car Crash J., **46**, pp. 145–164.

[2] Taylor P. A., and Ford C. C., 2009, "Simulation of blast-induced early-time intracranial wave physics leading to traumatic brain injury," J. Biomech. Eng., **131**(6), p. 061007.

[3] Pan Y., Shreiber D. I., and Pelegri A. A., 2011, "A Transition Model for Finite Element Simulation of Kinematics of Central

Nervous System White Matter," Biomed. Eng. Ieee Trans., **58**(12), pp. 3443 –3446.
[4] "CDC - Statistics - Traumatic Brain Injury - Injury Center" [Online]. Available: http://www.cdc.gov/traumaticbraininjury/statistics.html. [Accessed: 02-Jun-2012].
[5] Lipton P., 1999, "Ischemic Cell Death in Brain Neurons," Physiol. Rev., **79**(4), pp. 1431–1568.
[6] O'Brien J. ., 1990, "Shear-induced platelet aggregation," The Lancet, **335**(8691), pp. 711–713.
[7] Sheriff J., Bluestein D., Girdhar G., and Jesty J., 2010, "High-Shear Stress Sensitizes Platelets to Subsequent Low-Shear Conditions," Ann. Biomed. Eng., **38**(4), pp. 1442–1450.
[8] Wurzinger L. J., Opitz R., Blasberg P., and Schmid-Schönbein S.-S., 1985, "Platelet and coagulation parameters following millisecond exposure to laminar shear stress.," Thromb. Haemost., **54**(2), p. 381.
[9] Heinsen H., and Heinsen Y. L., 1983, "Cerebellar capillaries," Anat. Embryol. (Berl.), **168**(1), pp. 101–116.
[10] White J. G., and Clawson C. C., 1980, "Overview Article: Biostructure of Blood Platelets," Ultrastruct. Pathol., **1**(4), pp. 533–558.
[11] Zhao H., and Shaqfeh E. S. G., 2011, "Shear-induced platelet margination in a microchannel," Phys. Rev. E, **83**(6), p. 061924.
[12] Fung Y. C., 1993, Biomechanics: Mechanical Properties of Living Tissues, Springer.
[13] Bagchi P., 2007, "Mesoscale Simulation of Blood Flow in Small Vessels," Biophys. J., **92**(6), pp. 1858–1877.
[14] Tata D. ., and Anderson B. ., 2002, "A new method for the investigation of capillary structure," J. Neurosci. Methods, **113**(2), pp. 199–206.
[15] Nagayama K., Mori Y., Motegi Y., and Nakahara M., 2006, "Shock Hugoniot for Biological Materials," Shock Waves, **15**(3-4), pp. 267–275.
[16] Nyein M., Jerusalem A., Radovitzky R., Moore D., and Noels L., 2008, Modeling Blast-Related Brain Injury.
[17] Trudnowski R. J., and Rico R. C., 1974, "Specific Gravity of Blood and Plasma at 4 and 37 °C," Clin. Chem., **20**(5), pp. 615–616.
[18] Martin J. F., Plumb J., Kilbey R. S., and Kishk Y. T., 1983, "Changes In Volume And Density Of Platelets In Myocardial Infarction," Br. Med. J. (Clin. Res. Ed.), **287**(6390), pp. 456–459.
[19] McGrath B., Mealing G., and Labrosse M., 2011, "A mechanobiological investigation of platelets," Biomech. Model. Mechanobiol., **10**(4), pp. 473–484.
[20] Haga J. H., Beaudoin A. J., White J. G., and Strony J., 1998, "Quantification of the Passive Mechanical Properties of the Resting Platelet," Ann. Biomed. Eng., **26**(2), pp. 268–277.
[21] Kaster T., Sack I., and Samani A., 2011, "Measurement of the hyperelastic properties of ex vivo brain tissue slices," J. Biomech., **44**(6), pp. 1158–1163.
[22] Ichihara K., Taguchi T., Shimada Y., Sakuramoto I., Kawano S., and Kawai S., 2001, "Gray matter of the bovine cervical spinal cord is mechanically more rigid and fragile than the white matter," J. Neurotrauma, **18**(3), pp. 361–367.
[23] Miller K., and Chinzei K., 2002, "Mechanical properties of brain tissue in tension," J. Biomech., **35**(4), pp. 483–490.
[24] Dao M., Lim C. T., and Suresh S., 2003, "Mechanics of the human red blood cell deformed by optical tweezers," J. Mech. Phys. Solids, **51**(11–12), pp. 2259–2280.
[25] Suresh S., Spatz J., Mills J. P., Micoulet A., Dao M., Lim C. T., Beil M., and Seufferlein T., 2005, "Connections between single-cell biomechanics and human disease states: gastrointestinal cancer and malaria," Acta Biomater., **1**(1), pp. 15–30.
[26] Evans E. A., 1973, "New Membrane Concept Applied to the Analysis of Fluid Shear- and Micropipette-Deformed Red Blood Cells," Biophys. J., **13**(9), pp. 941–954.
[27] Mills J. P., Qie L., Dao M., Lim C. T., and Suresh S., 2004, "Nonlinear elastic and viscoelastic deformation of the human red blood cell with optical tweezers," Mech. Chem. Biosyst. Mcb, **1**(3), pp. 169–180.
[28] Cokelet G. R., and Meiselman H. J., 1968, "Rheological comparison of hemoglobin solutions and erythrocyte suspensions," Science, **162**(3850), pp. 275–277.
[29] Kang I., Panneerselvam D., Panoskaltsis V. P., Eppell S. J., Marchant R. E., and Doerschuk C. M., 2008, "Changes in the Hyperelastic Properties of Endothelial Cells Induced by Tumor Necrosis Factor-α," Biophys. J., **94**(8), pp. 3273–3285.
[30] Cullen D. K., Simon C. M., and LaPlaca M. C., 2007, "Strain rate-dependent induction of reactive astrogliosis and cell death in three-dimensional neuronal–astrocytic co-cultures," Brain Res., **1158**, pp. 103–115.
[31] Jérusalem A., and Dao M., 2012, "Continuum modeling of a neuronal cell under blast loading," Acta Biomater., **8**(9), pp. 3360–3371.